Interpretation of coupling impedance bench measurements

H. Hahn

Brookhaven National Laboratory, Upton, New York 11973, USA

(Received 24 September 2003; published 5 January 2004)

Coupling impedance values of accelerator components can be obtained from standard bench measurements based on the coaxial wire method. Longitudinal impedance is obtained with one wire and the transverse impedance with a twin wire inserted into the "device under test." The coupling impedance follows from the interpretation of the scattering coefficients from a network analyzer. In this paper, models and formulas applicable to the interpretation of the data are collected and reviewed. The paper is focused on lumped and distributed kicker magnets, for which a simulated measurement is numerically analyzed with the results graphically presented. This study suggests that the application of the standard lumped formula or the simple log formula for distributed impedances is appropriate.

DOI: 10.1103/PhysRevSTAB.7.012001 PACS numbers: 29.27.Bd

I. INTRODUCTION

The driving terms of instabilities in accelerators/storage rings always depend on the beam surroundings which are conveniently described by impedances [1,2]. Establishing and maintaining a coupling impedance budget becomes an important part of designing a high current accelerator. Theoretical estimates for typical accelerator components have been developed and are available in the standard literature [3–5]. For critical devices, the estimates need to be confirmed by impedance bench measurements [6]. The basic concept of bench measurements relies on simulating the beam by a wire for longitudinal or a twin wire Lecher line for transverse measurements. The measurements typically involve a measurement of the device under test (DUT) and of a reference structure with the difference or ratio of the data used to interpret the coupling impedance.

Coupling impedance bench measurements discussed here are performed with a network analyzer which provides the scattering coefficients, S_{21} and S_{11}, of the DUT and the reference. The standard formulas used to interpret the measured data were all derived in the framework of transmission line theory. The field configuration on an ideal transmission line is a TEM wave with purely transverse components. The finite wall conductivity or a geometrical wall disturbance change the field into a mode with a local axial component of the electric field responsible for the interaction with the beam. The assumption in the transmission line theory is, however, that the analysis can be performed with ideal walls and the real situation is handled by appropriately modifying the characteristic impedance and propagation constant. At a sufficient distance away from the device, the pure TEM mode is reestablished but with modified amplitude and phase of the scattering coefficients.

The question of to what degree the bench impedance is a valid representation of the beam impedance requires a separate analysis [7] and is beyond the scope of this paper, although certain results of the field analysis [8] are used here for error estimates. Theoretical and experimental [9] work suggest that agreement between actual and measured impedance can be achieved which is sufficient for the design requirements of accelerator/storage rings if several caveats are respected.

Wire measurements represent an ultrarelativistic beam, and the results need correction for lower energies [10]. Measurements of single lumped elements and even more so of distributed impedances are intrinsically perturbative and thus require the highest characteristic impedance of the reference tube and the smallest wire size, only limited by the signal-to-noise ratio. For the purpose of coupling impedance measurements, it is necessary to employ devices with beam tubes attached as part of the unit. End effects, i.e., the local appearance of evanescent modes, at the junction of the device and the transmission line is part of the impedance, thus extraneous steps in the transmission line must be avoided. End effects can to some degree be represented by added capacitive elements [11]. It is also plausible that the relative contribution of end effects is smaller for long distributed impedances than for lumped impedances. Obviously, the bench measurements are limited to the low frequency range where higher order modes do not propagate. Notwithstanding its limitations, transmission line analysis represents the proper framework for the interpretation of coupling impedance bench measurements. The general aspects of impedance bench measurements are discussed in [12] and need not be repeated here.

The R&D and design work for the construction of the Spallation Neutron Source (SNS) required detailed impedance studies of various components [13,14]. The transverse impedance of the extraction kickers was judged to be critical to the performance of the accumulator ring and received special attention [15]. The measured data is obtained from the network analyzer as a normalized ratio $S_{21}^{\mathrm{DUT}}/S_{21}^{\mathrm{REF}} = S_{21N}$ which is translated via a model to the Z^{DUT}. In the longitudinal measurement with a single wire, this represents already the coupling

impedance. In the measurement with twin wires, spaced apart by Δ, the transverse coupling impedance follows from

$$Z_\perp = \frac{c}{\omega\Delta^2} Z^{\mathrm{DUT}}. \tag{1}$$

The interpretation of the measurements was complicated by some inconsistencies of the available publications and pointed to the need for a uniform treatment. In this paper, the relevant models and the applicable interpretation are presented in general terms. The discussion starts with the lumped model for a longitudinal impedance and is extended to the transverse impedance model of a lumped kicker magnet. Then the model of a transmission line kicker magnet is developed and several formulas intended for a distributed wall impedance are collected and discussed. Finally, the theoretical forward scattering coefficients of prototypical models of a lumped kicker and of a transmission line kicker magnet are in a simulated wire measurement numerically interpreted via the various formulas. The simulated impedances are graphically represented and the appropriate formula choice is discussed. The results point to the standard Hahn and Pedersen (HP) formula [16] for lumped and to the simple Walling *et al.* [17] log formula as appropriate for the interpretation of the wire measurements.

II. LUMPED IMPEDANCE

The scattering coefficients due to a single, lumped wall impedance, Z_W , are well known in the transmission line framework and are repeated here for convenience:

$$S_{11} = \frac{Z_W}{2R_C + Z_W} \quad \text{and} \quad S_{21} = \frac{2R_C}{2R_C + Z_W}, \tag{2}$$

with R_C the characteristic impedance of the reference. Although in principle either coefficient gives correct results, the forward scattering coefficient is applicable to more general configurations and is generally preferred. The effect of the attached beam tubes is eliminated by normalizing the data with impedance, S_{21}^{DUT}, to that of a reference tube of equal length, S_{21}^{REF}. The wall impedance is given by the standard HP formula [16]

$$Z_W = 2R_C\left(\frac{S_{21}^{\mathrm{REF}}}{S_{21}^{\mathrm{DUT}}} - 1\right). \tag{3}$$

In the literature [18], an alternate expression, the Palumbo and Vaccaro (PV) formula [19] (also known as Sands and Rees) is found:

$$Z_W = 2R_C\left(1 - \frac{S_{21}^{\mathrm{DUT}}}{S_{21}^{\mathrm{REF}}}\right). \tag{4}$$

A derivation of both "lumped" formulas, based on the field equivalent principle and the reciprocity theorem, was published by Argan *et al.* [20] without arriving at a preference for either of them. Being of some academic interest, an estimate of their error is obtained by applying the formulas to the theoretical forward scattering coefficient from the wire measurement of a lumped impedance with the value Z_W. The integral field analysis yields in the "low frequency, small wire" limit the approximation for the normalized forward scattering coefficient [8]

$$\frac{S_{21}^{\mathrm{DUT}}}{S_{21}^{\mathrm{REF}}} \approx 1 - \frac{Z_W}{2R_C} + \frac{5}{4}\left(\frac{Z_W}{2R_C}\right)^2. \tag{5}$$

The interpretation via Eq. (3) yields $Z_{\mathrm{HP}} = Z_W(1 - Z_W/8R_C)$ and via Eq. (4) $Z_{\mathrm{PV}} = Z_W(1 - 5Z_W/8R_C)$, indicating a smaller error for the HP formula. Note also that the network analyzer uses this interpretation for the through impedance.

A. Resistive matching

In the application of the above formulas it is assumed that the characteristic impedance R_C of the reference wire/beam tube is fully matched to the network analyzer impedance R_0. Matching can be achieved by an ideal transformer or, with some loss in signal strength, by resistive matching. Resistive matching is achieved on the input side with a parallel resistor R_P plus a series resistor R_{in} with

$$\begin{aligned} R_P &= R_0\sqrt{R_C/(R_C - R_0)}, \\ R_{\mathrm{in}} &= R_C - R_0 R_P/(R_0 + R_P) \end{aligned} \tag{6}$$

and a series resistor on the output side, $R_{\mathrm{out}} = R_C - R_0$.

B. Effect of mismatch

Matching is typically imperfect and the finite length of the beam tubes leads to errors at higher frequencies. Formal expressions for the forward scattering coefficient associated with a series impedance Z between unmatched coaxial beam tubes are derived here from elementary circuit theory without the explicit use of hybrid matrices. The notation used is shown in Fig. 1.

The forward scattering coefficient is defined as

$$S_{21} = 2v_3/u \tag{7}$$

and is obtained by sequential elimination of the currents and voltages as follows [21]:

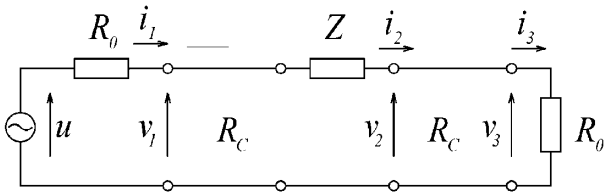

FIG. 1. Circuit model for wire impedance measurements.

$$S_{21} = -\frac{ZZ_1}{(Z+Z_2)(R_0+Z_1)} + \frac{Z_1(Z+Z_2)}{(Z+Z_2)(R_0+Z_1)}\cos 2k\ell - j\frac{Z_C(Z+2Z_2)}{(Z+Z_2)(R_0+Z_1)}\sin 2k\ell, \quad (8)$$

with

$$Z_1 = \frac{Z + Z_2 + jR_C\tan k\ell}{1 + (Z+Z_2)R_C^{-1}\tan k\ell};$$
$$Z_2 = \frac{R_0 + jR_C\tan k\ell}{1 + R_0R_C^{-1}\tan k\ell}. \quad (9)$$

The complete expression for the scattering coefficient is obtained via the MAXIMA program but it is too large for presentation here. The Taylor expansion for low frequencies, $k = \omega/c$, follows as

$$S_{21} \approx \frac{2R_0}{2R_0+Z} - j4k\ell\frac{R_0(R_0^2 + R_C^2 + R_0Z)}{R_C(2R_0+Z)^2}. \quad (10)$$

The coefficient ratio for the interpretation of the measurements yields the formula

$$\frac{S_{21}^{\mathrm{DUT}}}{S_{21}^{\mathrm{REF}}} \approx \frac{2R_0}{2R_0+Z} + j2k\ell\frac{Z}{R_C}\frac{R_C^2 - R_0^2}{(2R_0+Z)^2}, \quad (11)$$

which can be used to interpret the measurements. In practice, it gives only an estimate of the error due to a mismatch. Here R_0 represents the nominal instrument impedance (after matching) and R_C the actual line impedance. Note that toward zero frequency the error vanishes and consequently the nominal R_0, rather than the actual R_C which is less accurate, should be used in the HP formula.

III. LUMPED KICKER MAGNET

A. Nassibian and Sacherer (NS) model

The interpretation of wire measurements on a kicker magnet differs if the unit is designed as transmission or lumped magnet. The lumped magnet is at low frequencies characterized by a position-independent bus-bar current. In spite of its finite length, the lumped magnet can thus be analyzed with the help of a transformer model as developed in the seminal paper by Nassibian and Sacherer (NS) [22]. The illustrative example assumes a perfect magnet with ℓ, h, w, representing length, height, and width, respectively. The kicker has an inductance $L_K = \mu_0 h\ell/w$ and is terminated with the power supply impedance Z_g. The expression for the coupling impedance seen by the beam is

$$Z_\perp^{\mathrm{NS}} = \frac{c}{h^2}\frac{\omega L_K^2}{j\omega L_K + Z_g} = \frac{c}{h^2}\left\{\frac{\omega L_K^2 \mathrm{Re}Z_g}{\mathrm{Re}Z_g^2 + (\omega L_K + \mathrm{Im}Z_g)^2} - j\frac{\omega L_K^2(\omega L_K + \mathrm{Im}Z_g)}{\mathrm{Re}Z_g^2 + (\omega L_K + \mathrm{Im}Z_g)^2}\right\}, \quad (12)$$

with h the aperture in kick direction. In addition to the impedance coupled to the kicker termination, the beam sees an uncoupled impedance from image currents on the bus bar and the ferrite core. The uncoupled impedance is essentially inductive and the resistive part can often be neglected. An estimate for the uncoupled inductance L_I is obtained from the simple model of a dipole current between metal plates spaced apart by the width w corresponding to [15]

$$Z_\perp \approx \frac{j\pi\ell}{6w^2}Z_0. \quad (13)$$

B. Lumped kicker bench measurement

The transverse coupling impedance is obtained from a twin wire bench measurement in which the magnet is coupled to the twin wire transmission line by the mutual inductance M. The line has a nominal wire spacing Δ, a characteristic impedance of R_C, and is assumed fully matched to the network analyzer impedance. The line in the reference tube has the inductance $L_C = R_C\ell/c$ and a negligible resistance at the low frequencies of interest here. The wire measurements are interpreted with regard to a model represented by the equivalent circuit in Fig. 2. This model incorporates the impedance contributions from the uncoupled and coupled impedances, as well as that attributed to the leakage flux, $(1-\kappa^2)L_K$. The coupling coefficient κ and transformer ratio n are given by

$$\kappa = \sqrt{\frac{M^2}{L_K L_C}} \quad \text{and} \quad n = \frac{M}{L_K} = \frac{\Delta}{h}. \quad (14)$$

From the standard electrical engineering description of a transformer follows the forward scattering coefficient directly as

$$S_{21}^{\mathrm{DUT}} = 2R_C\left\{2R_C + n^2\frac{j\omega L_K Z_g}{j\omega L_K + Z_g} + j(1-\kappa^2)\omega L_C + j\omega L_I\right\}^{-1} = 2R_C\left\{2R_C + \frac{\omega^2 M^2}{j\omega L_K + Z_g} + j\omega L_C + j\omega L_I\right\}^{-1}. \quad (15)$$

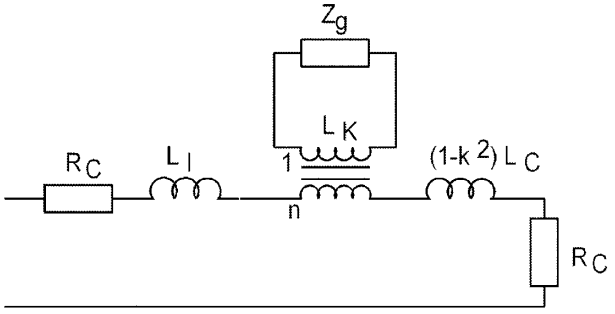

FIG. 2. Lumped kicker magnet circuit model.

The scattering coefficient of the reference line in the beam tube is in the low frequency approximation

$$S^{\mathrm{REF}} = 2R_C(2R_C + j\omega L_C)^{-1}. \tag{16}$$

The interpretation of the wire measurement via the lumped HP or PV formula yields, in an approximation to first order in R_C,

$$Z^{\mathrm{DUT}} = n^2 \frac{\omega^2 L_K^2}{j\omega L_K + Z_g} + j\omega L_{I,} \tag{17}$$

and the transverse coupling impedance (in kick direction) becomes

$$Z_\perp = \frac{c}{\omega}\frac{Z^{\mathrm{DUT}}}{\Delta^2} = \frac{c}{h^2}\frac{\omega L_K^2}{j\omega L_K + Z_g} + j\frac{c}{\Delta^2}L_I. \tag{18}$$

As expected, the wire measurement yields the theoretical Nassibian and Sacherer impedance estimate plus the uncoupled image impedance.

C. Davino and Hahn (DH) model

The measurement accuracy is increased by reducing the wire thickness which leads to an increase of the line inductance L_C. At constant wire spacing the transformer ratio n remains unchanged, but the coupling coefficient κ is reduced. In a typical setup, one has $\kappa^2 \ll 1$, leading to the expression for the coupled impedance

$$\begin{aligned} Z_\perp^{\mathrm{DH}} &= \frac{c}{\omega h^2}\frac{j\omega L_K Z_g}{j\omega L_K + Z_g} \\ &= \frac{c}{\omega h^2}\left\{\frac{(\omega L_K)^2 \mathrm{Re}Z_g}{\mathrm{Re}Z_g^2 + (\omega L_K + \mathrm{Im}Z_g)^2} + j\ldots\right\}, \end{aligned} \tag{19}$$

with the instability driving resistive part identical to the NS value. The Davino and Hahn (DH) model [15] differs from the NS model only in the reactive component.

Kicker magnets with access to the bus bar offer the possibility to short it, $Z_g = 0$, and use the shorted magnet as reference. Using the shorted magnet as reference simplifies and shortens the time between measurements and effectively eliminates instrument drift.

D. Reference calibration

The above interpretation of the measurements implies the calibration of the twin line to obtain S_{21}^{REF} in a beam tube with a diameter equal to the aperture of the magnet. The calibration can also be done in free space, which is simpler in the case of rigid lines, although it may be difficult to find a true free space. However, the line inductance (and correspondingly the characteristic impedance) from free-space tube beam tube with radius w is reduced by

$$\Delta L \approx \frac{2\mu_0 \ell}{\pi}\left(\frac{\Delta}{w}\right)^2. \tag{20}$$

The results from measurements based on the tube as reference will differ from that in air by the reactive transverse impedance per unit length [23]

$$Z_\perp^{\mathrm{pc}} = -j\frac{2}{\pi w^2}Z_0, \tag{21}$$

with $Z_0 = c\mu_0$, as long as radiation from the line in air and wall losses of the perfect conductive (pc) tube are negligible. It is to be noted that the instability driving resistive part does not change with the reference taken as tube or air.

E. Frequency effect

The current induced voltage in the magnet is $u_K \approx j\omega M i_C$ if the magnet length is short compared to the wavelength on the transmission line, but at higher frequencies one finds [22]

$$u_K = j\omega\{MG\}i_C \quad \text{with } G = \frac{\sin\frac{1}{2}k\ell}{\frac{1}{2}k\ell} \tag{22}$$

leading to the measured impedance of the kicker magnet,

$$Z^{\mathrm{DUT}} \approx \frac{(\omega MG)^2}{(Z_g + j\omega L_K)} + \ldots \tag{23}$$

and a corresponding correction of the measured transverse impedance.

IV. DISTRIBUTED IMPEDANCE

The transmission line analysis of a distributed impedance of length ℓ can be based on the Faltens *et al.* [6] model in which the total impedance of the device Z is represented by a uniformly distributed wall impedance Z/ℓ. The bench wire measurements are interpreted by comparing the wave propagation through the device with that in a "perfect" reference tube. In this model, propagation in the device is described by the changed characteristic impedance and propagation constants,

$$\begin{aligned} Z_W = \eta Z_C = Z_C\sqrt{1 - j\frac{Z}{\Theta Z_C}} \quad \text{and} \\ k_W = \eta k = k\sqrt{1 - j\frac{Z}{\Theta Z_C}}, \end{aligned} \tag{24}$$

where $\Theta = k\ell = \omega\ell/c$ and Z_C are the electric length and the characteristic impedance of the reference tube. In this model, the coupling impedance is fully described by the changed propagation constant k_W or through the single complex value η. The expression for the coupling impedance can now be formally written as

$$Z = j\Theta Z_C(k_W^2 - k^2)/k^2 \tag{25}$$

or alternatively by

$$Z = j\Theta Z_C(\eta + 1)(\eta - 1). \tag{26}$$

Representing the amplitude of the forward and reflected

wave by A and B, respectively, one can apply field matching (i.e., voltage and current matching in the transmission line) which leads to the conditions [24], at the input port of the wall impedance,

$$\begin{aligned} A_{\text{in}} + B_{\text{in}} &= A_{\text{DUT}} + B_{\text{DUT}}, \\ (A_{\text{in}} - B_{\text{in}}) &= (A_W - B_W)/\eta, \end{aligned} \tag{27}$$

at the output port ($A_{\text{out}} = 0$),

$$\begin{aligned} A_W e^{-j\eta\Theta} + B_W e^{j\eta\Theta} &= B_{\text{out}}, \\ (A_W e^{-j\eta\Theta} - B_W e^{j\eta\Theta})/\eta &= B_{\text{out}}. \end{aligned} \tag{28}$$

With the scattering coefficients defined as

$$S_{21} = \frac{B_{\text{out}}}{A_{\text{in}}} \quad \text{and} \quad S_{11} = \frac{B_{\text{in}}}{A_{\text{in}}} \tag{29}$$

one finds after simple manipulations

$$\begin{aligned} S_{21} &= \frac{4\eta e^{-j\eta\Theta}}{(\eta+1)^2 - (\eta-1)^2 e^{-j2\eta\Theta}} \\ &= \frac{2\eta}{2\eta\cos\eta\Theta + j(\eta^2+1)\sin\eta\Theta}, \end{aligned} \tag{30}$$

$$\begin{aligned} S_{11} &= \frac{(\eta^2-1)(1-e^{-j2\eta\Theta})}{(\eta+1)^2 - (\eta-1)^2 e^{-j2\eta\Theta}} \\ &= \frac{j(\eta^2-1)\sin\eta\Theta}{2\eta\cos\eta\Theta + j(\eta^2+1)\sin\eta\Theta}. \end{aligned} \tag{31}$$

These equations are exact within the limitations of the model and either of them could be used to extract numerically the value of η for use in Eq. (26). This task is simplified by combining the values of forward and reflected scattering coefficients to form the relation

$$\eta = \frac{1}{\Theta}\arccos\frac{1 - S_{11}^2 + S_{21}^2}{2S_{21}}. \tag{32}$$

Together with Eq. (26), this expression provides an exact value for the impedance but, due to its complexity, is of limited value for the routine interpretation of measurements. Furthermore, it was noted that insertion of the scattering coefficients for lumped elements from Eq. (2) into Eq. (32) leads to an undetermined solution of the form $\eta \to 0/0$.

A. Wang and Zhang (WZ) formula

An alternate formula for the interpretation of the wire measurements was derived by Wang and Zhang (WZ) [25] who introduced a corrected S_{21} parameter, $S_C \equiv e^{-jk_W\ell}$, obtained from

$$S_C^2 + \frac{S_{11}^2 - S_{21}^2 - 1}{S_{21}} S_C + 1 = 0. \tag{33}$$

This solution is confirmed by inserting $S_C = e^{-j\eta\Theta}$ into Eq. (33), which leads directly to the original Eq. (32). The propagation constants $k_W\ell = j\log S_C$ and $kl = j\log S_{21}^{\text{REF}}$ are combined with Eq. (25) to yield the expression

$$Z^{\text{WZ}} = -Z_C \ln\left(\frac{S_c}{S_{21}^{\text{REF}}}\right)\left(1 + \frac{\ln S_c}{\ln S_{21}^{\text{REF}}}\right). \tag{34}$$

This expression is exact, but due to the mathematics involved in finding S_C also of limited practical use.

B. Walling *et al.* log formula

Taking the ratio of scattering coefficients provided by the network analyzer, and treating the wall impedance as a perturbation of the reference tube, i.e., $Z \ll Z_C$, leads to

$$\begin{aligned} \frac{S_{21}^{\text{DUT}}}{S_{21}^{\text{REF}}} &= \frac{4\eta e^{-j(\eta-1)\Theta}}{(\eta+1)^2 - (\eta-1)^2 e^{-j2\eta\Theta}} \\ &\approx \exp[-j(\eta-1)\Theta]. \end{aligned} \tag{35}$$

Approximating Eq. (26) by

$$\eta - 1 \approx -j\frac{Z}{2\Theta Z_C}$$

results in the well-known log formula for distributed impedances by Walling *et al.* [17]:

$$Z = -2Z_C \ln\frac{S_{21}^{\text{DUT}}}{S_{21}^{\text{REF}}}. \tag{36}$$

C. Improved log formulas by Vaccaro and Jensen

Under the assumption that the reflection coefficient is small, $S_{11} \approx 0$, Vaccaro makes the approximation that $S_{21}^{\text{DUT}} \approx \exp(-jk_W\ell)$. Using Eq. (25), rather than (26), an improved expression for the measured impedance can be obtained [26,27],

$$Z = -Z_C \ln\left(\frac{S_{21}^{\text{DUT}}}{S_{21}^{\text{REF}}}\right)\left(1 + \frac{\ln S_{21}^{\text{DUT}}}{\ln S_{21}^{\text{REF}}}\right). \tag{37}$$

An identical equation, although written in a more convenient form by means of $S_{21}^{\text{REF}} = \exp(-j\Theta)$, was recently presented by Jensen [28],

$$Z = -2Z_C \ln\left(\frac{S_{21}^{\text{DUT}}}{S_{21}^{\text{REF}}}\right)\left\{1 + \frac{j}{2\Theta}\ln\left(\frac{S_{21}^{\text{DUT}}}{S_{21}^{\text{REF}}}\right)\right\}. \tag{38}$$

The improved impedance expressions require the knowledge of the electrical length of the device under test and one would expect that its accuracy decreases for shorter devices due to the signal noise. In contrast, the simple log formula is generally applicable including lumped components, provided that no strong resonance is present and the perturbation treatment is justified. The standard lumped impedance formula is applicable to single resonances and

has the advantage that the scattering coefficient ratio is directly converted into an impedance by the network analyzer. A more detailed comparison of the interpretation formulas is obtained from numerical simulations and will be presented in the sequel below.

V. TRAVELING WAVE KICKER

One of the more important examples of a distributed impedance is provided by traveling wave kicker magnets, and the interpretation of their bench measurements is typically done with the log formula. The above concept of treating the lumped kicker magnet as a transformer can be generalized and applied to traveling wave kickers [29]. The kicker properties are characterized by its characteristic impedance Z_K, propagation constant k_K, and electrical length, $\Theta_K = k_K \ell$. The kicker and the twin wire Lecher line are treated as transmission lines, coupled via the mutual inductance M for which the differential equations are well known. The general solution becomes unwieldy and several simplifications can be adopted without reducing the value of the results. The major part of the impedance is due to the coupled flux between the beam and the external terminations at either end of the bus bar, so that the contribution of the uncoupled flux can be neglected. In order to let the twin wire line represent the "stiff" ultrarelativistic beam, its current is considered externally imposed and thus unchanged by the current in the bus bar. The impedance seen by the beam is then obtained by the voltage generated by the bus-bar current via the mutual inductance. One finds, with the time dependence $e^{j\omega t}$ suppressed, the following set of differential equations in the position dependent variables i_K, u_K, i_B, u_B representing the kicker current and voltage, and the beam current and voltage, respectively,

$$\frac{\partial u_K}{\partial s} = -jk_K Z_K i_K + j\frac{\Delta}{h} k_K Z_K i_B, \tag{39}$$

$$\frac{\partial i_K}{\partial s} = -j\frac{k_K}{Z_K} u_K, \tag{40}$$

$$\frac{\partial u_B}{\partial s} = j\frac{\Delta}{h} k_K Z_K i_K, \tag{41}$$

where $k_K = k\sqrt{L'C'}$, $Z_K = \sqrt{L'/C'}$, and $k = \omega/c$. L' and C' are the kicker inductance and capacity per unit length and $\Delta/h = M'/L'$. Assuming an ultrarelativistic beam current, $i_B = Ie^{-jks}$, associated with the dipole strength $I\Delta$, one finds the impedance measured in the bench measurement

$$Z^{\mathrm{DUT}} = -\frac{1}{I}\int_0^\ell \frac{\partial u_B}{\partial s} e^{jks}. \tag{42}$$

This value yields the transverse coupling impedance according to

$$Z_\perp = \frac{c}{\omega\Delta^2} Z^{\mathrm{DUT}}. \tag{43}$$

The solution of the above differential equations is found by imposing the boundary conditions established by the kicker input and output terminations, R_i and R_o,

$$u_K(0) = R_i i_K(0), \qquad u_K(\ell) = -R_o i_K(\ell). \tag{44}$$

The general expression for the coupling impedance is somewhat lengthy, but reduces in typical kickers where $k \ll k_K$ to a manageable size. Furthermore, in the low frequency range of interest, one can take $i_B \approx I$. The case of input and output terminated with the characteristic impedance follows in this approximation as

$$Z_\perp = \frac{c}{\omega h^2} Z_K[(1 - \cos\Theta_K) + j(\Theta_K - \sin\Theta_K)], \tag{45}$$

which differs from Nassibian's expression [30]

$$Z_\perp^{\mathrm{NS}} = \frac{c}{\omega w^2} Z_K[(1 - \cos\Theta_K) + j(\Theta_K - \sin\Theta_K)] \tag{46}$$

only in its dependence on geometry.

VI. NUMERICAL SIMULATION OF WIRE MEASUREMENT

As illustration for the interpretation of wire measurements, the various available formulas are applied to the two prototypical examples of lumped and transmission line kicker magnets. The lumped example is modeled after the SNS extraction kicker magnet and the transmission line example after the RHIC injection kicker magnet. The frequency range covers 30 kHz to 100 MHz, corresponding to the actual measurements. The simulated measurement is obviously without instrument noise and drift, allowing the identification of smallest differences in the interpretative formulas used.

In the lumped case, the procedure consists in numerically "measuring" the forward scattering coefficient, Eq. (2),

$$S_{21}^{\mathrm{DUT}} = \frac{2R_C}{2R_C + Z}$$

for a representative impedance, Z, such as the DH kicker magnet model

$$Z = \frac{j\omega L_K Z_g}{j\omega L_K + Z_g},$$

with $Z_g = (R_g^{-1} + j\omega C_B)^{-1}$. The reference value is $S_{21}^{\mathrm{REF}} = 1$ and the normalized S_{21N} is interpreted via the various lumped as well transmission line formulas.

The transmission line case proceeds correspondingly, starting with Eq. (30),

$$S_{21} = \frac{2\eta}{2\eta\cos\eta\Theta + j(\eta^2 + 1)\sin\eta\Theta},$$

where $\eta = k\sqrt{1 - j(Z/\Theta R_C)}$ and $Z = Z_K[(1 - \cos\Theta_K) + j(\Theta_K - \sin\Theta_K)]$. The reference value is here

$S_{21}^{\mathrm{REF}} = e^{-j\Theta}$ and the normalized S_{21N} is numerically interpreted via the various formulas.

A. The lumped kicker magnet

The numerical data for the example of a resonant lumped device are taken from the open SNS extraction magnet: $L_K = 1\ \mu\mathrm{H}$, $C_B = 32$ pF, $R_g = 250\ \Omega$, and $R_C = 250\ \Omega$. The example of a nonresonant element corresponds to the SNS extraction magnet with the termination changed to $R_g = 25\ \Omega$. The results for the two examples are shown in Figs. 3 and 4, respectively.

In Fig. 3, the HP formula renders the original values and confirms only the absence of numerical errors. The PV formula departs significantly from the original values at the resonance frequency where $Z/R_C \approx 1$. The log formula, which is not intended for lumped devices, also exhibits errors but is more accurate than the PV formula. Clearly, the Vaccaro and Jensen (VJ) formula, Eq. (37), is not suited for lumped impedances with values reaching $Z/R_C \approx 1$.

The interpretation in Fig. 4 of an impedance with values $Z/R_C \ll 1$, that is the condition assumed in the perturbation treatment, is correctly done by all with the exception of the VJ formulas.

B. Transmission line magnet

The numerical data for the distributed impedance example is taken from the 1 m long RHIC injection magnet with $Z_K = 25\ \Omega$ and $R_C = 250\ \Omega$. The simulated data for the transmission line magnet is shown in Fig. 5. The black curve provided the scattering data and thus represents the WZ formula, but this was not numerically verified. Obviously, the HP formula is intended only for lumped elements and fails, i.e., provides negative results at higher frequencies. Walling's simple log formula shows the smallest errors for the instability driving resistive part of the impedance, whereas the "improved" VJ formula shows significant errors in the resistive part and is only better in the reactive part of the impedance. This result is contrary to an observation by Caspers [31] who states that the improved formula gives better results "at least for the real part." (In fact, a sign change of the corrective term in Eq. (38) led to better agreement with the real part at the expense of a degraded imaginary part, suggesting the use of the complex conjugate of the corrective term.) Thus, the properties of the VJ formula deserve a more detailed study before its routine application.

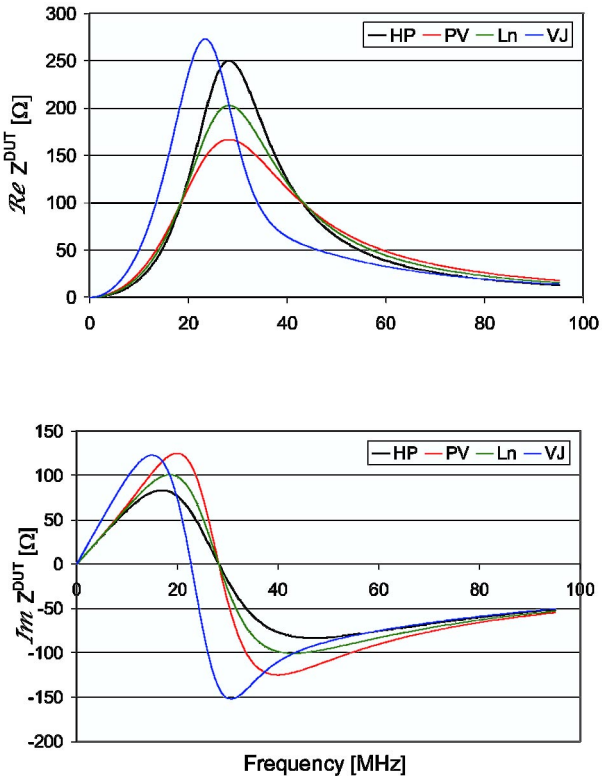

FIG. 3. (Color) Open kicker magnet. Interpretation of S21 via the HP (black), PV (red), log (green), and VJ (blue) formulas.

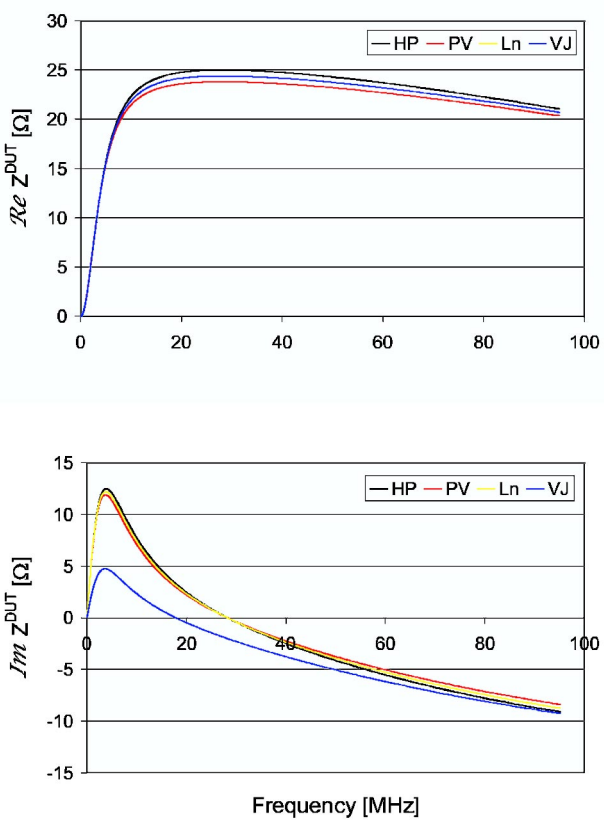

FIG. 4. (Color) Terminated kicker magnet. Interpretation of S21 via the HP (black), PV (red), log (yellow), and VJ (blue) formulas.

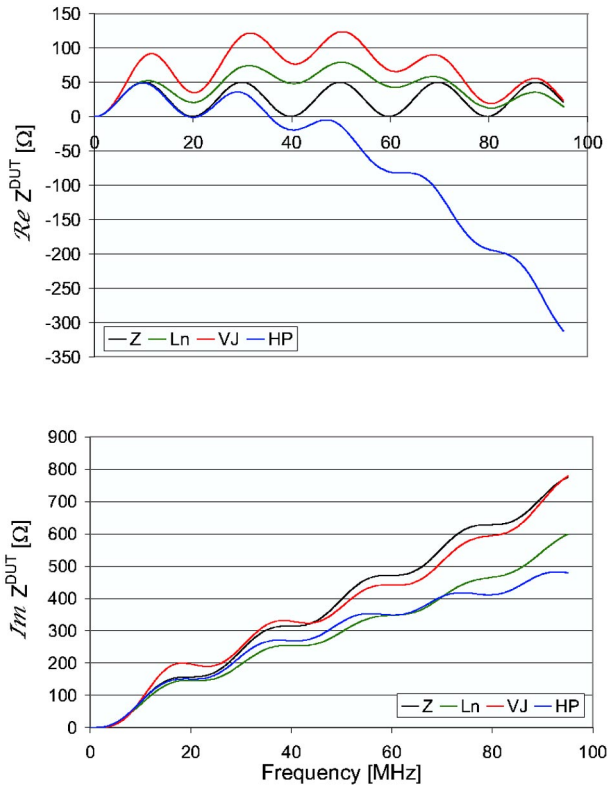

FIG. 5. (Color) Transmission line magnet. The black curve provides the scattering coefficient and is the reference impedance. The interpretation of S21 is via the log (green), VJ (red), and HP (blue) formulas.

VII. CONCLUSION

It is recognized that the three examples are not full justification for an all encompassing generalization. However, the examples are sufficiently representative of actual devices seen in accelerators/storage rings to give confidence for a conclusion. The numerical results can be summarized by stating that the use of the standard HP formula for lumped components and the simple log formula for distributed components provides an appropriate and, in view of measuring errors, adequate interpretation of the wire bench measurements.

ACKNOWLEDGMENTS

This work was accomplished under the auspices of the U.S. Department of Energy.

[1] V. G. Vaccaro, CERN Report No. ISR-RF 66-35, 1966.
[2] A. Sessler, CERN Yellow Report No. 67-2, 1967.
[3] G. Lambertson, in *Physics of Particle Accelerators*, edited by Melvin Month and Margaret Dienes, AIP Conf Proc. No. 153 (AIP, New York, 1987), Vol. 2, p. 1413.
[4] K. Y. Ng, in *Handbook of Accelerator Physics and Engineering*, edited by A. W. Chao and M. Tigner (World Scientific, Singapore, 1998), p. 203.
[5] K. Y. Ng, in *Physics of Particle Accelerators*, edited by Melvin Month and Margaret Dienes, AIP Conf. Proc. No. 184 (AIP, New York, 1989), Vol. 1, p. 472.
[6] A. Faltens, E. C. Hartwig, D. Mohl, and A. M. Sessler, in *Proceedings of the Eightth Internatiional Conference on High-Energy Accelerators, Geneva, 1971* (CERN, Geneva, 1971), p. 338.
[7] R. L. Gluckstern and R. Li, in *Proceedings of the 14th International Conference on High Energy Accelerators, Tsukuba, Japan, 1989*, edited by Y. Kimuro, K. Muto, H. Nakayama, and S. Ozaki [Part. Accel. 29, 159 (1990)].
[8] H. Hahn, Phys. Rev. ST Accel. Beams **3**, 122001 (2000).
[9] D. Davino, M. R. Masullo, V. G. Vaccaro, and L. Verolino, Nuovo Cimento Soc. Ital. Fis. **114B**, 1319 (1999).
[10] R. L. Gluckstern and A. V. Fedotov, in *Workshop on Instabilities of High Intensity Hadron Beams in Rings*, edited by T. Roser and S. Y. Zhang, AIP Conf. Proc. No. 496 (AIP, New York, 1999), p. 77.
[11] R. W. P. King, in *Encyclopedia of Physics*, edited by S. Fluegge (Springer-Verlag, Berlin, 1958), Vol. XVI, Chap. 17, p. 210.
[12] F. Caspers, in *Handbook of Accelerator Physics and Engineering* (Ref. [4]), p. 570.
[13] J. Wei, in *Proceedings of the European Particle Conference, Paris, 2002* (CERN, Geneva, 2002), p. 1067.
[14] H. Hahn, M. M. Blaskiewicz, and D. Davino, in Proceedings of the Particle Accelerator Conference, Portland, OR, 2003, RPPB010 (to be published).
[15] D. Davino and H. Hahn, Phys. Rev. ST Accel. Beams **6**, 012001 (2003).
[16] H. Hahn and F. Pedersen, BNL Report No. BNL 50870, 1978.
[17] L. S. Walling, D. E. Murray, D. V. Neuffer, and H. A. Thiessen, Nucl. Instrum. Methods Phys. Res., Sect. A **281**, 433 (1989).
[18] B. W. Zotter and S. A. Kheifets, *Impedances and Wakes in High-Energy Particle Accelerators* (World Scientific, Singapore, 1998), Chap. 11.3.1, p. 320.
[19] L. Palumbo and V. G. Vaccaro, Laboratori Nazionali di Frascati (LNF) Report No. LNF-89/035(P), 1989.
[20] A. Argan, L. Palumbo, M. R. Masullo, and V. G. Vaccaro, in *Proceedings of the Particle Accelerator Conference, New York, 1999,* edited by A. Luccio (IEEE, Pascataway, NJ, 1999), p. 1599.
[21] H. Hahn, BNL/SNS Technical Note No. 120.
[22] G. Nassibian and F. Sacherer, Nucl. Instrum. Methods **159**, 21 (1979).
[23] A. Mostacci, F. Caspers, and U. Iriso, in Proceedings of the Particle Accelerator Conference, Portland, OR, 2003, TPPB090 (to be published).
[24] H. Hahn, M. Morvillo, and A. Ratti, BNL Report No. AD/RHIC/RD-95, 1995.
[25] J. G. Wang and S. Y. Zhang, Nucl. Instrum. Methods Phys. Res., Sect. A **459**, 389 (2001).
[26] V. G. Vaccaro, INFN Report No. INFN/TC-94/023, 1994.
[27] M. Cardito, G. Di Massa, F. Gallucio, R. Losito, M. R. Masullo, and V. G. Vaccaro, in *Proceedings of the*

Particle Accelerator Conference, Washington, DC, 1993, edited by C.W. Leemann and J. J. Bisognano (IEEE, Piscataway, NJ, 1993), p. 2154.
[28] E. Jensen, CERN PS/RF/Note No. 2000-001, 2000.
[29] H. Hahn, in *Workshop on Instabilities of High Intensity Hadron Beams in Rings*, (Ref. [10]), p. 266.
[30] G. Nassibian, CERN Report No. CERN/PS 84-25(BR); CERN Report No. CERN-PS 85-68(BR), 1984.
[31] F. Caspers, in *Tenth Workshop on LEP-SPS Performance, Chamonix, France, 2000* (CERN, Geneva, 2000), pp. 85–93.